Asian Journal of Chemistry; Vol. 37, No. 8 (2025), 1873-1878

ASIAN JOURNAL OF CHEMISTRY

https://doi.org/10.14233/ajchem.2025.34080

1,4-Disubstituted-1,2,3-triazole Linked Cyclic Ketones as Cytotoxic Agents

SUBHAS S. KARKI[1,2,*], BASAVARAJ METIKURKI[3,†], ARNIKA DAS[1,2,†], ASHOK MADARAKHANDI[1], ARNAV KUMAR[1,2], SUJEET KUMAR[3] and DOMINIQUE SCHOLS[4]

[1]Department of Pharmaceutical Chemistry, KLE College of Pharmacy, 2nd Block, Rajajinagar, Bengaluru-560010, KLE Academy of Higher Education and Research, Belagavi-590010, India
[2]Dr. Prabhakar B. Kore Basic Science Research Centre, Off-Campus, Bengaluru-560010, India
[3]Department of Pharmaceutical Chemistry, Nitte College of Pharmaceutical Sciences, Nitte (Deemed to be University), Yelahanka, Bengaluru-560064, India
[4]Rega Institute for Medical Research, Department of Microbiology, Immunology and Transplantation, Laboratory of Virology and Chemotherapy, KU Leuven, B-3000 Leuven, Belgium
[†]Authors contributed equally

*Corresponding author: E-mail: subhasskarki@gmail.com; subhashskarki@klepharmblr.org

Received: 19 May 2025; *Accepted*: 29 June 2025; *Published online*: 31 July 2025; AJC-22064

A series of 1,2,3-triazole-linked cyclic ketones (**AR 1-14**) were synthesized involving the condensation of triazole-aldehydes with cyclic ketones in tetrahydrofuran and potassium hydroxide. The synthesized derivatives were evaluated for their *in vitro* cytotoxicity against retinal (hTERT RPE-1)-1), pancreatic (Capan-1), myeloid (K-562, Hap-1), colorectal (HCT 116), lung (NCI-H460), lymphoblastic (DND-41) and non-Hodgkin lymphoma (Z-138) cells. Among the tested derivatives, compound 2,6-*bis*(4-((1-(4-fluorobenzyl)-1*H*-1,2,3-triazol-4-yl)-methoxy)benzylidene)cyclohexanone (**AR-7**) exhibited moderate cytotoxic property with an IC_{50} of 11.8 μM and 13.6 μM against pancreatic adenocarcinoma and colorectal carcinoma cells, respectively. Molecular docking against galectin-1 receptor (PDB ID: 4Y24) demonstrated a favourable binding interaction (-7.1 kcal/mol) indicating a strong receptor-ligand affinity.

Keywords: 1,2,3-Triazole, Cytotoxicity, Galectin-1 (4Y24), Molecular docking.

INTRODUCTION

In India, the estimated number of new cancer cases in 2022 was 14,61,427 and one in nine individuals is likely to develop cancer during their lifetime. Alarmingly, the incidence of cancer cases in the country is projected to increase by 12.8% by 2025 [1]. In recent decades, heterocyclic chemistry has played a pivotal role in the discovery and development of new anticancer agents. Among heterocycles, nitrogen-containing frameworks are particularly valued due to their low toxicity, enhanced reactivity and strong receptor affinity [2]. Considering this, the present study focuses on the design and development of novel 1,2,3-triazole analogs with potential anticancer activity. It was synthesized *via* a 1,3-dipolar cycloaddition reaction between an azide and an alkyne, under metal-catalyzed or metal-free conditions [3]. It is widely employed in medicinal chemistry as a bioisostere due to its chemical stability and favourable pharmacokinetic properties [4].

Galectins are the promising molecular targets in cancer therapy representing a family of β-galactoside-binding soluble lectins composed of approximately 130 amino acids. These proteins are distributed throughout the cytosol and nucleus, where they mediate various biological functions *via N*- or *O*-glycosylation, interacting with carbohydrate recognition domains (CRDs) [5-8]. Out of the 15 identified galectins, galectin-1 has garnered significant attention due to its overexpression in several cancers, where it plays a key role in metastasis, tumor progression and immune-evasion. It binds to glycosylated receptors (such as glycoproteins like CD45, CD43 or integrins) on the surface of immune cells, particularly T cells, dendritic cells and natural killer (NK) cells [9-12]. These characteristics make galectin-1 an appealing molecular target for the design of novel anticancer therapeutics.

EXPERIMENTAL

All reagents and solvents were of analytical grade and used as received unless otherwise stated. The purity of reagents and solvents was confirmed prior to use. The progress of reactions was monitored by thin layer chromatography (TLC) using pre-coated Aluchrosep silica gel 60/UV254 plates (Sd Fine-Chem Ltd.). Melting point was determined using the open capillary tube method in heavy liquid paraffin and were reported uncorrected. Fourier transform infrared (FTIR) spectra were recorded using the diffuse reflectance technique with IR-grade KBr on a JASCO 460+ spectrometer. The nuclear magnetic resonance (NMR) spectra were obtained using Bruker Ultraspec AMX 400 and JEOL RESONANCE spectrometers operating at 400 (^{1}H NMR) and 500 (^{13}C NMR) MHz in deuterated DMSO and chloroform. The chemical shift (δ) values were reported in ppm relative to tetramethylsilane (TMS) as an internal standard.

The intermediates 4-(prop-2-ynyloxy)benzaldehyde (**3**), benzyl azide (**4a**), 4-nitrobenzyl azide (**4b**), 4-methylbenzyl azide (**4c**), 4-chlorobenzyl azide (**4d**) and the 4-((1-benzyl-1*H*-1,2,3-triazol-4-yl)methoxy)benzaldehydes (**5a-h**)were synthesized as per literature [13]. Compounds 4-fluoro (**4e**), 4-methoxy (**4f**), 3,5-dimethoxy (**4g**) and 3,4,5-trimethoxybenzyl azide (**4h**) were synthesized according to literature reference.

Synthesis of (2*E*,6*E*)-2,6-*bis*(4-((1-benzyl-1*H*-1,2,3-triazol-4-yl)methoxy)benzylidene) cyclic ketones (AR 1-14): A solution of triazole aldehyde (**5a-h**, 1 mmol) in THF (20 mL) was mixed with an equal molar volume of a methanolic KOH solution (20 mL). To this mixture, the corresponding cyclic ketone (**6** or **7**, 1 mmol) was added gradually with continuous stirring and stirred at 35 ºC for 16 h. Progress of reaction was monitored by TLC. Upon completion, the reaction mixture was poured into cold water and neutralized with dilute HCl. The resulting precipitate was filtered, washed with cold water and recrystallized from an ethanol-chloroform mixture (80:20 v/v) to yield **AR1-14**.

(2*E*,6*E*)-2,6-*Bis*(4-((1-benzyl-1*H*-1,2,3-triazol-4-yl)-methoxy)benzylidene)cyclohexanone (AR-1): Yellow crystals, 70% yield. m.p.: 160-162 ºC. IR (KBr, ν_{max}, cm^{-1}): 3061, 3007, 2945, 2729, 1655, 1596, 1558, 1455, 1297. ^{1}H NMR (400 MHz, DMSO-d_6) δ ppm: 8.29 (2H, s, triazole-H), 7.57 (2H, s, benzyl-H), 7.52 (4H, d, *J* = 8.8 Hz, Ar.), 7.39-7.30 (10H, m, Ar.), 7.15 (4H, d, *J* = 8.8 Hz, Ar.), 5.61 (4H, s, 2 × -OCH$_2$-), 5.19 (4H, s, 2 × -NCH$_2$-), 2.87 (4H, t, 2 × -CH$_2$-), *J* = 10.4 Hz), 1.71 (2H, p, -CH$_2$-, *J* = 24 Hz).

(2*E*,6*E*)-2,6-*Bis*(4-((1-(4-methoxybenzyl)-1*H*-1,2,3-triazol-4-yl)methoxy)benzylidene) cyclohexanone (AR-2): Yellow amorphous powder, 55% yield, m.p.: 128-130 ºC. IR (KBr, ν_{max}, cm^{-1}): 3072, 3019, 2953, 2836, 1654, 1597, 1551, 1460, 1385, 1277. ^{1}H NMR (DMSO-d_6) δ ppm: 8.25 (2H, s, triazole-H), 7.58 (2H, s, benzyl-H), 7.52 (4H, d, *J* = 7.2 Hz, Ar.), 7.31 (4H, d, *J* = 6.8 Hz, Ar.), 7.12 (4H, d, *J* = 6.8 Hz, Ar.), 6.93 (4H, d, *J* = 6.8 Hz, Ar.) 5.53 (4H, s, 2 × -OCH$_2$-), 5.18 (4H, s, 2 × -N-CH$_2$-), 3.73 (6H, s, 2 × -OCH$_3$), 2.87 (4H, q, *J* = 10.4 Hz, 2 × -CH$_2$-), 1.73 (2H, p, -CH$_2$-, *J* = 19.2 Hz); ^{13}C NMR (500 MHz, DMSO-d_6) δ ppm: 188.62 (s), 159.15 (s), 158.49 (s), 142.68 (s), 135.37 (s), 134.36 (s), 132.22 (s), 131.53 (s), 129.64 (s), 127.90 (s), 124.47 (s), 114.84 (s), 114.13 (s), 113.90 (s), 61.15 (s), 55.13 (s), 52.40 (s), 27.91 (s), 22.46 (s) ppm.

(2*E*,6*E*)-2,6-*Bis*(4-((1-(3,5-dimethoxybenzyl)-1*H*-1,2,3-triazol-4-yl)methoxy)benzylidene)cyclohexanone (AR-3): Yellow crystals, 61% yield, m.p.: 115-118 ºC. IR (KBr, ν_{max}, cm^{-1}): 3076, 2998, 2840, 1661, 1596, 1560, 1466, 1352, 1295. ^{1}H NMR (400 MHz, DMSO-d_6) δ ppm: 8.29 (2H, s, triazole-H), 7.57 (2H, s, benzyl-H), 7.51 (4H, d, *J* = 9.2 Hz, Ar.), 7.12 (4H, d, *J* = 8.8 Hz, Ar.), 6.46-6.44 (6H, m, Ar.), 5.52 (4H, s, 2 × -OCH$_2$-), 5.20 (4H, s, 2 × -N-CH$_2$-), 3.70 (12H, s, 4 -OCH$_3$), 2.87 (4H, t, 2 × -CH$_2$, *J* = 10.8 Hz), 1.7 1 (2H, p, -CH$_2$-, *J* = 24.8 Hz).

(2*E*,6*E*)-2,6-*Bis*(4-((1-(3,4,5-trimethoxybenzyl)-1*H*-1,2,3-triazol-4-yl)methoxy)benzylidene)cyclohexanone (AR-4): Yellow crystals, 65% yield, m.p.: 180-184 ºC. IR (KBr, ν_{max}, cm^{-1}): 3094, 2996, 2798, 1666, 1591, 1508, 1465, 1387, 1246. ^{1}H NMR (400 MHz, DMSO-d_6) δ ppm: 8.30 (2H, s, triazole-H), 7.57 (2H, s, benzyl-H), 7.51 (4H, d, *J* = 8.8 Hz, Ar.), 7.11 (4H, d, *J* = 8.8 Hz, Ar.), 6.69 (4H, s, Ar.), 5.50 (4H, s, 2 × -OCH$_2$-), 3.72 (12H, s, 4 × -OCH$_3$), 3.62(6H, s, 2 × -OCH$_3$), 2.87 (4H, t, 2- CH$_2$, *J* = 10.8 Hz), 1.71 (2H, p, -CH$_2$-, *J* = 24.8 Hz).

(2*E*,6*E*)-2,6-*Bis*(4-((1-(4-nitrobenzyl)-1*H*-1,2,3-triazol-4-yl)methoxy)benzylidene)cyclohexanone (AR-5): Yellow crystals, 58% yield, m.p.: 180-182 ºC. IR (KBr, ν_{max}, cm^{-1}): 3086, 2982, 2714, 1660, 1598, 1558, 1345, 1455, 1464, 1229. ^{1}H NMR (400 MHz, DMSO-d_6) δ ppm: 8.37 (2H, s, triazole-H), 8.24 (4H, d, *J* = 8.4 Hz, Ar.), 7.57 (2H, s, benzyl-H), 7.54-7.47 (8H, m, Ar.), 7.12 (4H, d, *J* = 8.8 Hz, Ar.), 5.80 (4H, s, 2 × -OCH$_2$-), 5.22 (4H, s, 2 × -N-CH$_2$-), 2.86 (4H, t, 2 × -N-CH$_2$-, *J* = 10.4 Hz), 1.71 (2H, p, -CH$_2$-, *J* = 24.8 Hz); ^{13}C NMR (500 MHz, DMSO-d_6) δ ppm: 188.41 (s), 158.45 (s), 147.26 (s), 143.40 (s), 142.92 (s), 135.36 (s), 134.39 (s), 132.24 (s), 131.61 (s), 129.06 (s), 128.29 (s), 125.24 (s), 123.95 (s), 114.88 (s), 113.89 (s), 61.14 (s), 51.94 (s), 27.92 (s), 22.46 (s).

(2*E*,6*E*)-2,6-*Bis*(4-((1-(4-methylbenzyl)-1*H*-1,2,3-triazol-4-yl)methoxy)benzylidene)cyclohexanone (AR-6): Creamy crystals, 65% yield, m.p.: 148-150 ºC. IR (KBr, ν_{max}, cm^{-1}): 3096, 3027, 2946, 2877, 1654, 1595, 1557, 1456, 1420, 1294. ^{1}H NMR (400 MHz, DMSO-d_6) δ ppm: 8.25 (2H, s, triazole-H), 7.57 (2H, s, triazole H), 7.51(4H, d, *J* = 8.8 Hz, Ar.), 7.21 (4H, d, *J* = 8.0 Hz, Ar.), 7.17 (4H, d, *J* = 8.0 Hz, Ar.), 7.11 (4H, d, *J* = 8.8 Hz, Ar.), 5.54 (4H, s, 2 × -OCH$_2$-), 5.18 (4H, s, 2 × -N-CH$_2$-), 2.86 (4H, t, 2 × -CH$_2$-, *J* = 10.4 Hz), 2.27 (6H, s, 2 × -CH$_3$), 1.71 (2H, p, -CH$_2$). ^{13}C NMR (500 MHz, DMSO-d_6) δ ppm: 188.60 (s), 158.46 (s), 142.68 (s), 137.50 (s), 135.33 (s), 134.35 (s), 132.96 (s), 132.18 (s), 129.27 (s), 128.23 (s), 127.99 (s), 124.60 (s), 114.84 (s), 61.15 (s), 52.64 (s), 27.87 (s), 22.45 (s), 20.66 (s).

(2*E*,6*E*)-2,6-*Bis*(4-((1-(4-fluorobenzyl)-1*H*-1,2,3-triazol-4-yl)methoxy)benzylidene)cyclohexanone (AR-7): Yellow crystals, 67% yield, m.p.: 118-120 ºC. IR (KBr, ν_{max}, cm^{-1}): 3084, 3011, 2942, 2834, 1662, 1600, 1564, 1456, 1298. ^{1}H NMR (400 MHz, DMSO-d_6) δ ppm: 8.29 (2H, s, triazole-H), 7.57 (2H, s, benzyl-H), 7.52 (4H, d, *J* = 8.8 Hz, Ar.), 7.41-7.36 (4H, m, Ar.), 7.21 (4H, t, *J* = 16, Ar.), 7.11 (4H, d, *J* = 8.8 Hz, Ar.), 5.60 (4H, s, 2 × -OCH$_2$-), 5.19 (4H, s, 2 × -N-CH$_2$-), 2.87 (4H, t, 2 × -CH$_2$-, *J* = 10.4 Hz), 1.73 (2H, p, -CH$_2$, *J* = 24.8 Hz);

^{13}C NMR (500 MHz, DMSO-d_6) δ ppm: 188.99 (s), 163.66 (s), 161.57 (s), 159.05 (s), 143.36 (s), 135.94 (s), 134.98 (s), 132.79 (s), 130.93 (s), 130.87 (s), 128.84 (s), 125.29 (s), 116.28 (s), 116.11 (s), 115.45 (s), 61.73 (s), 52.63 (s), 28.48 (s), 23.04 (s).

(2*E*,6*E*)-2,6-*Bis*(4-((1-(4-chlorobenzyl)-1*H*-1,2,3-triazol-4-yl)methoxy)benzylidene)cyclohexanone (AR-8): Creamy crystals, 60% yield, m.p.: 188-190 ºC. IR (KBr, ν_{max}, cm^{-1}): 3082, 3004, 2962, 2837, 1698, 1598, 1513, 1464, 1255; ^{1}H NMR (400 MHz, DMSO-d_6) δ ppm: 8.26 (2H, s, triazole-H), 7.66 (4H, d, *J* = 7.2 Hz, Ar.), 7.40 (2H, s, benzyl-H), 7.31 (4H, d, *J* = 7.2 Hz, Ar.), 7.16 (4H, d, *J* = 7.2 Hz, Ar.), 6.93 (4H, d, *J* = 7.2 Hz, Ar.) 5.53 (4H, s, 2 × -OCH_2-), 5.20 (4H, s, 2 × -N-CH_2-), 3.73 (6H, s, 2 × -OCH_3), 3.05 (4H, s, 2 × -CH_2).

(2*E*,5E)-2,5-*Bis*(4-((1-(4-methoxybenzyl)-1*H*-1,2,3-triazol-4-yl)methoxy)benzylidene)cyclopentanone (AR-9): Creamy crystals, 58% yield, m.p.: 210-212 ºC. IR (KBr, ν_{max}, cm^{-1}): 3072, 3000, 2942, 2837, 1689, 1595, 1508, 1459, 1351, 1243. ^{1}H NMR (400 MHz, DMSO-d_6) δ ppm: 8.31 (2H, s, triazole-H), 7.65 (4H, d, *J* = 9.2 Hz, Ar.), 7.38 (2H, s, benzyl-H), 7.15 (4H, d, *J* = 9.2 Hz, Ar.), 6.66 (4H, s, Ar.), 5.50 (4H, s, 2 × -OCH_2-), 5.22 (4H, s, 2 × -N-CH_2-), 3.72 (12H, s, 4 × -OCH_3-), 3.62 (6H, s, 2 × -OCH_3), 3.04 (4H, s, 2 × -CH_2-); ^{13}C NMR (500 MHz, DMSO-d_6 δ ppm): 189.18 (s), 159.01 (s), 153.59 (s), 143.29 (s), 137.94 (s), 135.91 (s), 134.95 (s), 132.77 (s), 131.86 (s), 128.82 (s), 125.23 (s), 115.43 (s), 106.32 (s), 61.71 (s), 60.55 (s), 56.46 (s), 53.70 (s), 28.36 (s), 23.03 (s).

(2*E*,5E)-2,5-*Bis*(4-((1-(3,4,5-trimethoxybenzyl)-1*H*-1,2,3-triazol-4-yl)methoxy)benzylidene)cyclopentanone (AR-10): Brown crystals, 68% yield. m.p.: 138-140 ºC. IR (KBr, ν_{max}, cm^{-1}): 3095, 3025, 2958, 2711, 1652, 1593, 1552, 1455, 1351, 1295; ^{1}H NMR (400 MHz, DMSO-d_6 δ ppm: 8.26 (2H, s, triazole-H), 7.65 (4H, d, *J* = 8.8 Hz, Ar.), 7.39 (2H, s, benzyl-H), 7.22 (4H, d, *J* = 8.0 Hz, Ar.), 7.18 (4H, d, *J* = 8.0 Hz, Ar.), 7.15 (4H, d, *J* = 8.8 Hz, Ar.), 5.55 (4H, s, 2 × -OCH_2-), 5.20 (4H, s, 2 × -N-CH_2-), 3.05 (4H, s, 2 × -CH_2-), 2.27 (s, 6H, 2 × -CH_3); ^{13}C NMR (500 MHz, DMSO-d_6) δ ppm: 188.42 (s), 158.46 (s), 142.80 (s), 135.37 (s), 135.00 (s), 134.38 (s), 132.89 (s), 131.53 (s), 129.92 (s), 128.78 (s), 128.26 (s), 124.86 (s), 114.87 (s), 113.94 (s), 61.15 (s), 52.02 (s), 27.9 1(s), 22.47 (s).

(2*E*,5E)-2,5-*Bis*(4-((1-(4-methylbenzyl)-1*H*-1,2,3-triazol-4-yl)methoxy)benzylidene)cyclopentanone (AR-11): Yellow amorphous mass, % yield 72. m.p.: 208-210 ºC. IR (KBr, ν_{max}, cm^{-1}): 3082, 3034, 2989, 2875, 1697, 1632, 1597, 1457, 1377, 1286; ^{1}H NMR (400 MHz, DMSO-d_6 δ ppm): 8.37 (2H, s, triazole-H), 8.24 (4H, d, *J* = 8.8 Hz, Ar.), 7.66 (4H, d, *J* = 8.8 Hz, Ar.), 7.54 (4H, d, *J* = 8.8 Hz, Ar.), 7.39 (2H, s, benzyl-H), 7.16 (4H, d, *J* = 8.8 Hz, Ar.), 5.80 (4H, s, 2 × -OCH_2-), 5.24 (4H, s, 2 × -N-CH_2-), 3.05 (4H, s, 2 × -CH_2-); ^{13}C NMR (500 MHz, DMSO-d_6 δ ppm: 195.50 (s), 159.62 (s), 143.21 (s), 138.11 (s), 136.22 (s), 133.58 (s), 133.07 (s), 132.61 (s), 129.88 (s), 128.98 (s), 128.61 (s), 125.27 (s), 115.80 (s), 61.78 (s), 53.23 (s), 26.49 (s), 21.28 (s).

(2*E*,5E)-2,5-*Bis*(4-((1-(4-nitrobenzyl)-1*H*-1,2,3-triazol-4-yl)methoxy)benzylidene)cyclopentanone (AR-12): Yellow crystals, 65% yield, m.p.: 185-187 ºC. IR (KBr, ν_{max}, cm^{-1}): 3078, 2882, 2710, 1665, 1600, 1550, 1350, 1498, 1471, 1220; ^{1}H NMR (400 MHz, DMSO-d_6 δ ppm): 8.30 (2H, s, triazole-H), 7.66 (4H, d, *J* = 8.8 Hz, Ar.), 7.44 (4H, d, *J* = 9.2 Hz, Ar.), 7.39 (2H, s, benzyl-H), 7.34 (4H, d, *J* = 9.2 Hz, Ar.), 7.15 (4H, d, *J* = 9.2 Hz, Ar.), 5.62 (4H, s, 2 × -OCH_2-), 5.21 (4H, s, 2 × -N-CH_2-), 3.05 (4H, s, 2 × -CH_2).

(2*E*,5E)-2,5-*Bis*(4-((1-(4-chlorobenzyl)-1*H*-1,2,3-triazol-4-yl)methoxy)benzylidene)cyclopentanone (AR-13): Yellow amorphous, 58% yield, m.p.: 228-230 ºC. IR (KBr, ν_{max}, cm^{-1}): 3077, 3025, 2921, 2856, 1698, 1622, 1580, 1462, 1365, 1274; ^{1}H NMR (400 MHz, DMSO-d_6, δ ppm): 8.30 (s, 2H, triazole H), 7.66 (d, 4H, *J* = 8.8 Hz), 7.44 (d, 4H, *J* = 9.2 Hz), 7.39 (s, 2H, benzyl-H), 7.34 (d, 4H, *J* = 9.2 Hz), 7.15 (d, 4H, *J* = 9.2 Hz), 5.62 (s, 4H, 2 × -OCH_2-), 5.21 (s, 4H, 2 × -CH_2-), 3.05 (s, 4H, cyclopentanyl); ^{13}C NMR (400 MHz, DMSO-d_6, δ ppm: 159.01, 142.72, 135.65, 134.99, 132.89, 132.48, 132.02, 129.92, 128.78, 128.42, 124.89, 115.22, 61.19, 52.02, 25.91.

(2*E*,5E)-2,5-*Bis*(4-((1-(4-fluorobenzyl)-1*H*-1,2,3-triazol-4-yl)methoxy)benzylidene)cyclopentanone (AR-14): Yellow crystals, 59% yield, m.p.: 208-210 ºC. IR (KBr, ν_{max}, cm^{-1}): 3040, 2962, 2847, 1692, 1620, 1585, 1472, 1363, 1245; ^{1}H NMR (400 MHz, DMSO-d_6, δ ppm): 8.30 (s, 2H, triazole H), 7.66 (d, 4H, *J* = 8.8 Hz), 7.41-7.37 (m, 6H), 7.23-7.13 (td, 8H, *J* = 16, 8.8 Hz), 5.60 (s, 4H, 2 × -OCH_2-), 5.21 (s, 4H, 2 × -CH_2-), 3.05 (s, 4H, -CH_2-CH_2-); ^{13}C NMR (500 MHz, DMSO-d_6, δ ppm): 16.91, 159.05, 142.69, 135.63, 132.46, 130.34, 130.27, 124.72, 115.69, 115.52, 115.19, 61.39, 52.03, 25.89.

Bio-evaluation

Cell lines: The human cancer cell lines Capan-1, HCT-116, NCI-H460, Hap-1, K-562, Z-138 and non-cancerous hTERT RPE-1 were obtained from the American Type Culture Collection (ATCC, Manassas, VA, USA). The DND-41 cell line was sourced from the Deutsche Sammlung von Mikroorganismen und Zellkulturen (DSMZ Leibniz-Institut, Germany). All cell lines were cultured according to the suppliers' recommendations. Culture media were purchased from Gibco (Gibco Life Technologies, Belgium) and supplemented with 10% fetal bovine serum (HyClone, Cytiva, USA). For all the biological assays, the test compounds and reference drugs were dissolved in DMSO at a concentration of 100 μM.

Cytotoxicity assays: Adherent cell lines were seeded at densities ranging from 500 to 1500 cells per well in 384-well plates (Greiner Bio-One, Belgium). Following overnight incubation, the cells were treated with seven different concentrations of the test compounds, ranging from 100 to 0.006 μM. Untreated cell lines (*i.e.* without compound treatment) were used as negative controls. Suspension cell lines were seeded at densities ranging from 2500 to 5000 cells per well in 384-well culture plates containing the test compounds at the same concentration points. All cell lines were incubated for 72 h with compounds and then analyzed using the CellTiter 96® AQueous One Solution Cell Proliferation Assay reagent (Promega, The Netherlands) according to the manufacturer's instructions. Absorbance of the samples was measured at 490 nm using a SpectraMaxPlus 384 (Molecular Devices, USA) and OD values were used to calculate the 50% inhibitory concentration (IC_{50}). Compounds were tested in two independent experiments [14].

***In silico* study:** The binding interaction of the most active compound in the **AR-7** series with galectin-1 protein (PDB ID: 4Y24) was investigated using AutoDockVina 1.1.2. Prior to docking, the protein structure was prepared by removing water molecules, adding hydrogen atoms and assigning appropriate atom types and partial charges to each atom. The chemical structure of **AR-7** was constructed using ChemBioDraw Ultra 12.0 and its geometry was optimized using the MMFF94 force field. Energy minimization was carried out with a maximum of 1000 iterations and a root mean square (RMS) gradient threshold of 0.1 kcal/mol. The minimized structure was further prepared using the AutoDock Tools (ADT) package, where Gasteiger charges were assigned, hydrogens added and rotatable bonds were defined. Both ligand and receptor structures were saved in .pdbqt format, as required for docking. Docking was performed within a defined binding site using a grid box of 40 × 80 × 40 points with a grid spacing of 0.375 Å. The centre of the grid box was set at coordinates X = 22.081, Y = 0.3, Z = -16.435. The docking simulations were run on a Linux-based multicore CPU platform. Among the generated poses, the conformation with the lowest binding energy was selected and aligned to the active site of the receptor crystal structure for visualization and interaction analysis [15].

RESULTS AND DISCUSSION

Fourteen derivatives of 1,2,3-triazole-linked cyclic ketones (**AR1-14**) were synthesized as outlined in **Scheme-I.** The synthetic route commenced with the reaction of 4-hydroxybenzaldehyde (**1**) and propargyl bromide (**2**) in dry DMF yielding 4-(prop-2-ynyloxy)benzaldehyde (**3**). In the subsequent step, compound **3** was subjected to a copper (I)-catalyzed azide-alkyne cycloaddition (CuAAC) with different benzyl azides (**4a-h**) in the presence of sodium ascorbate and $CuSO{\cdot}5H_2O$, affording the corresponding triazole-benzaldehydes (**5a-h**). The final derivatives **AR1-14** were synthesized by condensation of **5a-h** with cyclic ketones **6** and **7** in THF and KOH.

The FTIR spectra of compounds **AR 1-14** had shown aromatic C-H stretching vibrations in the range of 3096-3000 cm^{-1}, while aliphatic C-H stretches appeared between 2998-2710 cm^{-1}. The carbonyl (C=O) stretching bands were noted between 1698-1652 cm^{-1}. The ^1H NMR spectra showed singlets for triazole ring protons between δ 8.37-8.25 ppm. The aromatic protons appeared in the range δ 8.24-6.44 ppm, while the benzylic protons were observed between δ 7.58-7.38 ppm. Methylene protons from $-OCH_2-$ and $-NCH_2-$ groups resonated in the ranges of δ 5.80-5.50 and δ 5.24-5.18 ppm, respectively. Methoxy ($-OCH_3$) protons were evident between δ 3.73-3.62 ppm in compounds **AR2, AR3, AR4, AR8 and AR9**. Methyl protons in **AR6** and **AR11** were identified as singlet at δ 2.27 ppm. Cycloalkyl protons resonated broadly in the range of δ 3.05-1.71 ppm. The ^{13}C NMR spectra data for the compounds had displayed peaks in the range of δ 195 to 188 ppm for -C=O of cyclic ketones, for aromatic carbons between δ 159-106 ppm and for methoxy and methyl carbons in the range of δ 62 to 21 ppm.

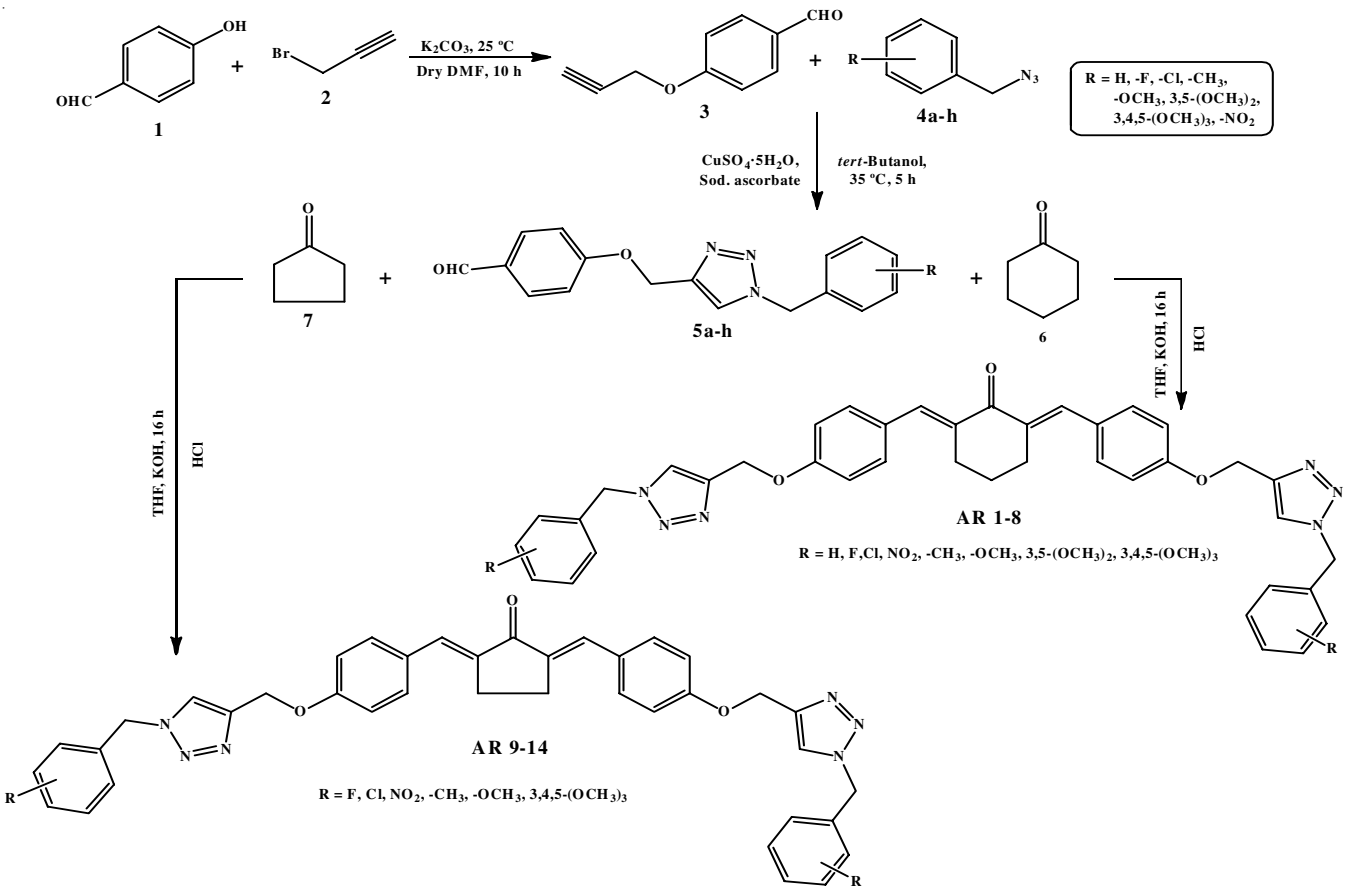

Scheme-I: Synthesis of 1,4-disubstituted-1,2,3-triazole linked cyclic ketones (**AR 1-14**)

Cytotoxic study: The *in vitro* cytotoxicity study was conducted on different human cancerous and non-cancerous (hTERT RPE-1) cell lines, following established protocols reported in the literature. Dimethyl sulfoxide (DMSO) was employed as the solvent control, while docetaxel and staurosporine were used as reference standards. The IC_{50} values, as summarized in Table-1, highlight compound **AR-7** as the moderately active molecule in the series, exhibiting an IC_{50} of 11.8 and 13.6 μM against the Capan-1 and HCT-116 cell lines, respectively while compound **AR-9** had shown IC_{50} of 17.4 μM against HCT-116 cells. In contrast to docetaxel and staurosporine, none of the other molecules were found to be more cytotoxic to non-cancerous hTERT RPE-1 cells, indicating a higher degree of selectivity for cancerous cells. Compounds **AR 1-3** were not tested during the study, hence not included in Table-1.

***In silico* study:** In support of *in vitro* cytotoxicity data, the binding mechanism of the most active compound **AR-7** was investigated using molecular docking approach. AutoDockVina 1.1.3 was employed to dock the molecule **AR-7** into the active site of the target protein, human galectin-1 (PDB ID: 4Y24). The co-crystallized ligand TD-139 (bound to galectin-1) was first extracted and prepared using AutoDock Tools. The prepared TD-139 ligand was re-docked into the binding pocket of galectin-1 using the same grid configuration applied for molecule **AR-7**. The re-docking of TD-139 yielded a conformation closely matching the crystal structure, with a docking score of -7.1 kcal/mol, thereby confirming the reliability of the docking methodology (Fig. 1). Subsequent docking of molecule **AR-7** revealed a favourable binding pose with a docking score of -7.6 kcal/mol, indicating a potentially stronger interaction compared to TD-139. The CRD of galectin-1 is comprised of five carbohydrate-binding sub-sites (CBS) designated A to E (Fig. 2). The co-ligand TD-139 was found to interact with sub-sites B, C, D and E, whereas molecule **AR-7**, due to its extended structure engaged with sub-sites A, B, C and E. Detailed interaction analysis concluded that (i) 4-fluorophenyl ring of compound **AR-7** formed an electrostatic interaction with Asp123 in sub-site A; (ii) the triazole ring exhibited a hydrophobic π-alkyl interaction with Val31 in sub-site B, Trp68 in sub-site C and an electrostatic interaction with His44 in sub-site C; (iii) the oxygen linker between the triazole and benzene rings participated in hydrogenbonding with His44; (iv) another triazole ring formed hydrogen bonding with Asp54 in sub-site A; and (v) finally, a fluorophenyl ring at the terminal end of the molecule established an electrostatic π-cation interaction with Arg73 in sub-site A (Fig. 3).

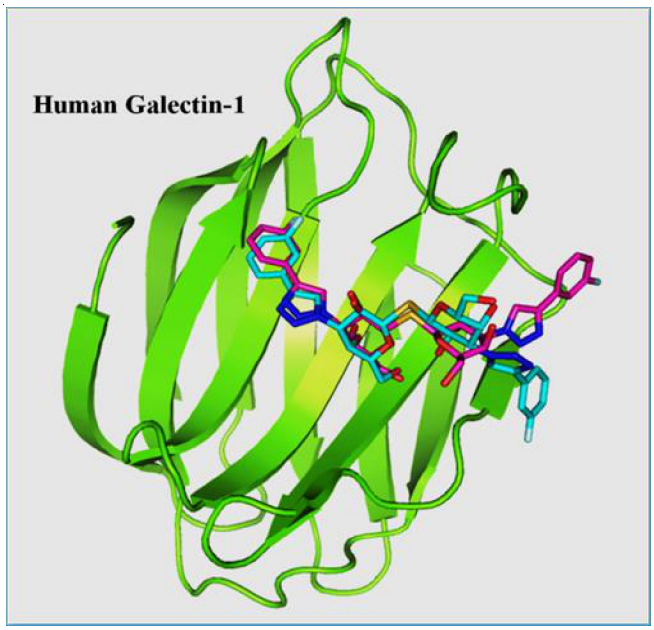

Fig. 1. Protein-co-crystal ligand (TD-139) against human galectin-1 (PDB ID: 4Y24). The co-crystallized ligand is shown in pink and its docked pose showed in cyan

Collectively, it can be summarized that compound **AR-7** interacted with all conserved residues in the CBS of galectin-1, similar to TD-139 involving three electrostatic, two hydrogen

TABLE-1
CYTOTOXICITY DATA (*in vitro*) OF SYNTHESIZED DERIVATIVES **AR4-14** AND REFERENCE MOLECULES DOCETAXEL AND STAUROSPORINE

Code	R	IC_{50}							
		hTERT RPE-1	Capan-1	Hap-1	HCT-116	NCI-H460	DND-41	K-562	Z-138
		Retina (non-cancerous)	Pancreatic adenocarcinoma	Chronic myeloid leukemia	Colorectal carcinoma	Lung carcinoma	Acute lymphoblastic leukemia	Chronic myeloid leukemia	Non-Hodgkin lymphoma
AR-4	3,4,5-tri-OCH_3	>100	78.2	89.7	39.9	>100	>100	>100	>100
AR-5	4-NO_2	>100	58.3	>100	47.3	24.7	>100	>100	>100
AR-6	4-CH_3	30.9	31.5	38.2	27.7	21.2	24.4	>100	>100
AR-7	4-F	38.1	11.8	31.6	13.6	21.9	>100	>100	>100
AR-8	4-Cl	>100	>100	>100	>100	>100	>100	>100	>100
AR-9	OCH_3	73.8	>100	84.3	17.4	76.7	>100	>100	>100
AR-10	3,4,5-tri-OCH_3	48.5	31.5	45.6	80.3	40.5	68.5	>100	>100
AR-11	4-CH_3	40.3	25.6	42.5	29.2	20.8	37.1	>100	>100
AR-12	4-NO_2	53.8	20.1	43.1	20.5	47.4	>100	>100	>100
AR-13	4-Cl	42.9	47.2	51.2	48.3	53.6	>100	>100	>100
AR-14	4-F	51.8	50	>100	67	58.1	>100	>100	40.8
Docetaxel (nM)		13.5	6.3	1.6	0.8	0.1	1.9	3.4	1.9
Staurosporine (nM)		0.4	4.6	0.3	0.3	3.2	6.4	29.8	0.3

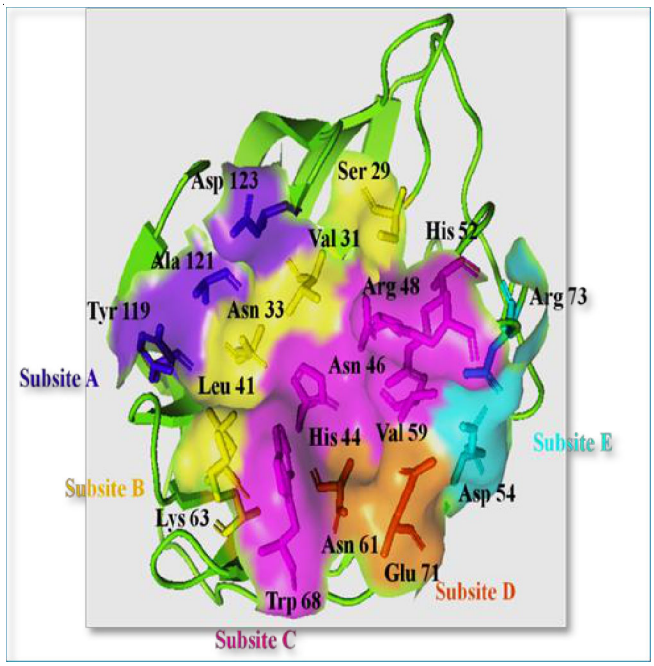

Fig. 2. The residue belonging to the 5 subsites in CBS of CRD in human galectin-1 is shown in surface and stick representation. Subsite A in purple, subsite B in yellow, subsite C in pink, subsite D in orange and subsite E in cyan

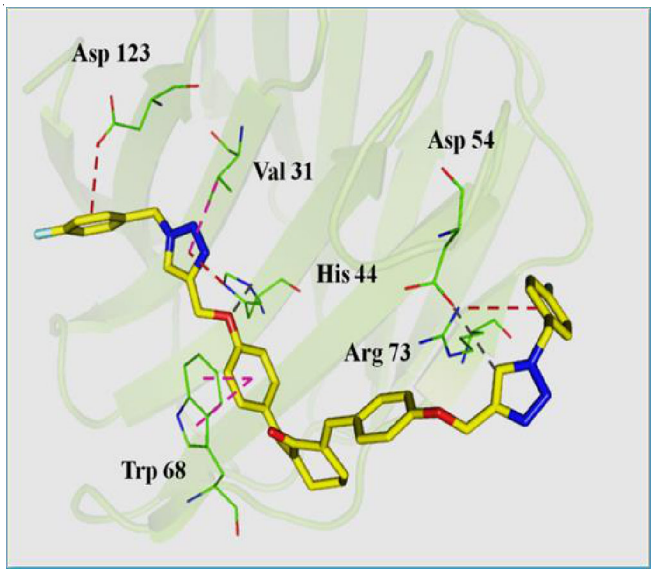

Fig. 3. Protein-AR-7 against human galectin-1 (PDB ID: 4Y24). The compound **AR-7** is shown in yellow sticks. Electrostatic, hudrogen and hydrophobic interactions are shown in orange, grey and pink dotted line respectively

bonding and two hydrophobic interactions, supporting its stronger binding affinity and potential for greater inhibition of galectin-1 compared to other synthesized molecules in the series.

Conclusion

A series of fourteen 1,2,3-triazole-linked cyclic ketones **(AR 1-14)** were synthesized and structurally characterized. Molecular docking was performed on galectin-1 (PDB ID: 4Y24) with TD-139 as the reference ligand. Among the synthesized derivatives, compound **AR-7** exhibited a docking score of -7.1 Kcal/mol comparable to that of TD-139 (-7.6 kcal/mol) indicating strong binding affinity toward the galectin-1 active site. Cytotoxicity screening was performed across eight human cell lines, including both cancerous and non-cancerous types. Compound **AR-7** demonstrated the highest inhibitory effect specifically against the Capan-1 pancreatic cancer cell line. However, none of the synthesized derivatives surpassed the cytotoxic efficacy of standard drugs docetaxel and staurosporine. These findings suggest that further structural optimization is required to enhance the anticancer potency of this scaffold.

ACKNOWLEDGEMENTS

The authors acknowledge to KLE College of Pharmacy and Dr. Prabhakar B. Kore, Basic Science Research Centre (Off-Campus), Bengaluru, India for the support to carryout this work.

CONFLICT OF INTEREST

The authors declare that there is no conflict of interests regarding the publication of this article.

REFERENCES

1. K. Sathishkumar, M. Chaturvedi, P. Das, S. Stephen and P. Mathur, *Indian J. Med. Res.*, **156**, 598 (2022); https://doi.org/10.4103/ijmr.ijmr_1821_22
2. A. Kumar, A.K. Singh, H. Singh, V. Vijayan, D. Kumar, S. Thareja, J.P. Yadav, J. Naik, P. Pathak, M. Grishina, A. Verma, H. Khalilullah, M. Jaremko, A.H. Emwas and P. Kumar, *Pharmaceuticals*, **16**, 299 (2023); https://doi.org/10.3390/ph16020299
3. D.P. Vala, R.M. Vala and H.M. Patel, *ACS Omega*, **7**, 36945 (2022); https://doi.org/10.1021/acsomega.2c04883
4. M.S. Malik, S.A. Ahmed, I.I. Althagafi, M.A. Ansari and A. Kamal, *RSC Med. Chem.*, **11**, 327 (2020); https://doi.org/10.1039/C9MD00458K
5. L. Johannes, R. Jacob and H. Leffler, *J. Cell Sci.*, **131**, 208884 (2018); https://doi.org/10.1242/jcs.208884
6. I. Camby, M. Le Mercier, F. Lefranc and R. Kiss, *Glycobiology*, **16**, 137R (2006); https://doi.org/10.1093/glycob/cwl025
7. F. Cedeno-Laurent and C.J. Dimitroff, *Clin. Immunol.*, **142**, 107 (2012); https://doi.org/10.1016/j.clim.2011.09.011
8. G. Rabinovich, *Br. J. Cancer*, **92**, 1188 (2005); https://doi.org/10.1038/sj.bjc.6602493
9. G. Emilsson, E. Röder, B. Malekian, K. Xiong, J. Manzi, F.-C. Tsai, N.-J. Cho, M. Bally and A. Dahlin, *Front Chem.*, **7**, 1 (2019); https://doi.org/10.3389/fchem.2019.00001
10. S.G. Nerella, *Eur. J. Med. Chem. Rep.*, **11**, 100170 (2024); https://doi.org/10.1016/j.ejmcr.2024.100170
11. J.M. Cousin and M.J. Cloninger, *Int. J. Mol. Sci.*, **17**, 1566 (2016); https://doi.org/10.3390/ijms17091566
12. Y. Huang, H.C. Wang, J. Zhao, M.H. Wu and T.C. Shih, *Biomolecules*, **11**, 1398 (2021); https://doi.org/10.3390/biom11101398
13. A. Das, G. Greco, S. Kumar, E. Catanzaro, R. Morigi, A. Locatelli, D. Schols, H. Alici, H. Tahtaci, F. Ravindran, C. Fimognari and S.S. Karki, *Comput. Biol. Chem.*, **97**, 107641 (2022); https://doi.org/10.1016/j.compbiolchem.2022.107641
14. T. Van de Walle, A. Theppawong, C. Grootaert, S. De Jonghe, L. Persoons, D. Daelemans, K. Van Hecke, J. Van Camp and M. D'hooghe, *Monatsh. Chem.*, **150**, 2045 (2019); https://doi.org/10.1007/s00706-019-02516-1
15. O. Trott and A.J. Olson, *J. Comput. Chem.*, **31**, 455 (2010); https://doi.org/10.1002/jcc.21334